Approaches to minimize overhang angles of SLM parts

Michael Cloots
Irpd AG, St.Gallen, Switzerland
Livia Zumofen
Center for Product and Process Development, ZHAW, Winterthur, Switzerland
Adriaan Bernardus Spierings
Institute for Rapid Product Development, inspire AG, St. Gallen, Switzerland
Andreas Kirchheim
Center for Product and Process Development, ZHAW, Winterthur, Switzerland, and
Konrad Wegener
Institute for machine tools and manufacturing IWF, ETH Zürich, Zurich, Switzerland

Abstract

Purpose – For geometries exhibiting overhanging surfaces, support structures are needed to dissipate process heat and to minimize geometrical distortions attributed to internal stresses. The use of support structures is often time- and cost-consuming. For this reason, this study aims to propose an approach which minimizes the use of such structures.

Design/methodology/approach – For minimizing the use of support structures, process parameters in combination with a contour-like exposure strategy are developed to realize support-less overhanging structures of less than 35°. These parameters are implemented in a shell-core strategy, which follows the idea of applying different processing strategies to the critical (overhanging) shell and the uncritical core of the part. Thereby, the core is processed with standard parameters, aiming a dense material. On the critical shell, optimized processing parameters are applied, reaching good results in terms of surface quality, especially at extreme overhang situations.

Findings – The results show that the selective laser melting (SLM) technology is able to realize support-less overhanging surfaces by choosing suitable scan strategies and process parameters. Particularly good results are always obtained when the exposure direction of the shell is parallel to the contour of the sample.

Originality/value – The validity of the results is demonstrated through the successful reproduction of the build strategy on two commercial SLM machines, reaching support-free builds of surfaces with an angle to the horizontal of less than or equal to 30°.

Keywords SLM, Overhanging surfaces, Part segmentation, Scan strategies, Support-less

Paper type Research paper

1. Introduction

Selective laser melting (SLM) is experiencing increasing attention in the field of industrial production. With this additive manufacturing technology, stainless steel (Averyanova and Bertrand, 2009), hot-work steel, aluminum (Buchbinder *et al.*, 2011), Ni-based alloys (Rickenbacher *et al.*, 2012) as well as other metal alloys have previously been successfully applied to SLM. But the high degree of geometric freedom, which is a unique feature of the additive manufacturing technologies, is limited by two process-specific effects independent of the material choice, namely, heat concentration and thermo-elastic distortion.

During the SLM process, locally high temperatures above the melting point of the metal material being processed occur. The process heat in the melt pool is almost completely dissipated by the already manufactured part of the component, as it is typical for laser-based processes with high energy densities (Gedda *et al.*, 2002). In case of disturbed heat conduction, support structures are build up and are connected to those zones of the part where heat dissipation is limited by the comparably very poor thermal conductivity of metal powder (Sih and Barlow, 2004). As stated by Wang *et al.* (2013), in most cases, heat conduction becomes critical where the angle between the overhanging surface and the top plane of the base plate is close to 45° or less, as for smaller angles, the isolating effect of the powder becomes more dominant. In that case, heat cannot be conducted successfully from the process plane. As a result of the isolating powder, the heat remains longer in the melt and the melt pool increases (Kruth

The current issue and full text archive of this journal is available on Emerald Insight at: **www.emeraldinsight.com/1355-2546.htm**

Rapid Prototyping Journal
23/2 (2017) 362–369

[DOI 10.1108/RPJ-05-2015-0061]

The authors would like to thank their colleague Alex Frauchiger who supported them with his profound knowledge in SLM.

Received 26 May 2015
Revised 31 December 2015
30 April 2016
Accepted 16 May 2016

et al., 2007). When the melt pool reaches a critical size, it is possible that the melt flows into the loose powder because of gravity and capillary forces and the thermal energy available leads to more powder particles being molten. In consequence, this results in an unacceptable surface quality and a loss of geometrical accuracy. This mechanism underlines the need of support structures, which offer a sufficient thermal conductivity to dissipate the heat as fast as possible.

The process heat is closely linked with another SLM-specific phenomenon. According to Chivel and Smurov (2010), the very rapid cooling of the melt leads to an extremely high temperature gradient of several thousand K/mm, resulting in residual stresses (Gusarov *et al.*, 2013; Mercelis and Kruth, 2006) . The residual stress within the SLM track accumulates track by track on the component level and leads to a significant residual stress situation in the whole part (Zaeh and Branner, 2010; Cloots *et al.*, 2013). Depending on the part geometry, this can lead to large distortions. In consequence, there is a need for support structures for overhanging surfaces and sub-structures of the part with an insufficient thermal inertia to dissipate the process heat and to counteract possible component distortion. However, manufacturing support structures has a direct impact on the productivity of the SLM process. The need for support structures increases the laser exposure time during the process. Furthermore, the removal of these structures is a significant cost driver. If there would be a possibility to minimize the need for support structures, this could contribute to a significant cost reduction. According to Wang *et al.* (2013), numerous factors having different impacts on the result of the smallest possible overhang angle could already be identified. These influence factors mentioned are directly linked to the volume energy E_V (Thijs *et al.*, 2010). So, overhang angles of less than 45° are only possible if the volume energy is lowered by adjusting the variable scan speed v_s, hatch distance h and layer thickness t_L. Wang *et al.* (2013) also mentioned the influence of the scan strategy, but its significance has not been analyzed.

2. Research objective

The objective of this study is derived from the general idea of segmenting a sample into a core and a shell part, to build up critical regions with specifically adapted process parameters to realize the best possible sample quality. For example, overhanging surfaces or horizontal holes are such critical regions within a part. The aim of this study is to define process parameters and scan strategies for shell structures of the so-called shell-core components made of SS316L, as illustrated in Figure 1 (right), to realize a minimum overhang angle without the need for any support structures. For this study, two tests have been conducted.

3. Machines and powders

3.1 Machines

The ConceptLaser M2 is equipped with a fiber laser, generating a beam at a wavelength of 1,070 nm in the continuous wave mode and at a maximum power of about 200 W. The beam has a measured M^2 of < 1.3 and a corresponding diameter of 100 μm (D4σ) in the focal plane (Gaussian mode). Nitrogen is used as the inert gas, and a flexible brush-like coating system is used.

Figure 1 Test Series 1: variable process parameters h, α and v_s that indicate the value range used for the design of experiments to determine φ_{min}; Test Series 2: shell-core sample for investigating the minimum shell-thickness $t_{s,min}$

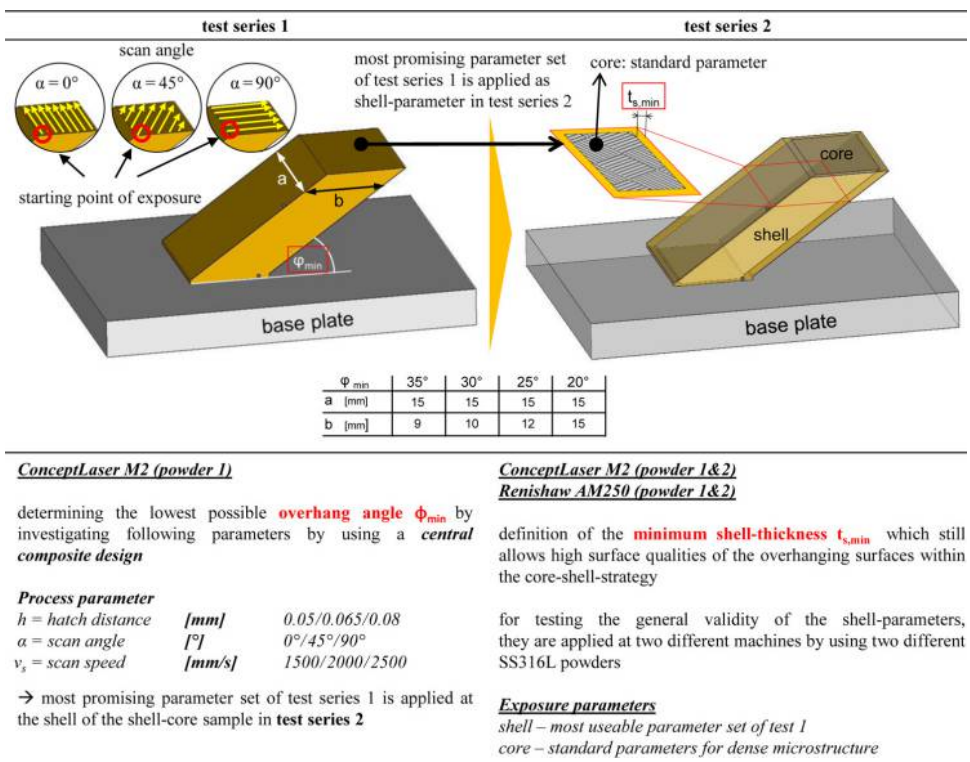

The Renishaw AM250 is used to figure out the general validity of the results worked out at the ConceptLaser M2. The Renishaw AM250 is also equipped with a fiber laser at 200 W. The beam has a M^2 of < 1.1. Argon is used as the inert gas, and the coating system of Renishaw was modified, but it still included a silicone lip. In contrast to the ConcepLaser M2, the laser of the Renishaw laser melting system operates in a pulsed mode.

3.2 Powders

Two austenitic SS316L powders with different particle size distribution are used for the tests. Powder 1, used during the Test Series 1 and 2, is produced by a gas atomizing of virgin cast material. The log-normal particle size distribution of Powder 1 is shown in Figure 2. The mean particle size of this powder is 13 μm. The volume fraction of those particles with a diameter of less than 13 μm is about 10 per cent of the total powder volume. The fraction of fine particles compared to Powder 2 is very high. This trend is confirmed by the scanning electron microscope (SEM) image in Figure 3, where the high proportion of fine powder particles of Powder 1 is clearly evident.

The average particle diameter of Powder 2 used in Test Series 2 is significantly larger than that of Powder 1. The mean diameter is about 24 μm. In addition, the bi-modal particle size distribution in Figure 2 points out the smaller proportion of fine particles. The SEM image in Figure 3 confirms this fact; only a small amount of fine particles are visible.

4. Experiments and methods

4.1 Test Series 1: analysis of process parameters and scan strategies for minimum overhang angle φ_{min}

The first test geometry is used to determine those processing parameters that will later be applied on the shell of the samples, as shown in Figure 1, allowing the additive manufacturing of minimum overhangs below. Thereby, the influence of the hatch distance h, scan angle α and scan speed v_s are investigated. The scan angle α will be varied in a way that the laser exposure runs parallel to the overhanging contour (= edge of the component, scan angle $\alpha = 0°$), perpendicular to the overhanging contour (scan angle $\alpha = 90°$) or a combination of both (scan angle $\alpha = 45°$), as graphically explained in Figure 1. Constant parameters are laser power at 200 W as well as the layer thickness of 30 μm. For all parameter combinations, the exposure of a layer always starts inside the sample and ends at the edge of the overhang. The exposure begins, therefore, always inside the sample to prevent excessive energy input at the edge of the sample where heat dissipation is difficult. The test series starts with an overhang angle of 35°. The tests are repeated each time with a 5° reduced overhang angle until no acceptable results occur.

The experimental field design of experiments (DOE) of Test Series 1, shown in Figure 4, is based on the central composite design (CCD), resulting in 16 test points for every tested overhang angle φ.

Because the overhang samples are not suitable for the Archimedes density measurement because of the geometry, cubic samples were produced under the same conditions to study the parameter-specific density, assuming that the density of a cubic sample is the same as that of the overhang samples.

The surface quality of the overhanging surfaces is determined by a tactile measurement of R_a. Because quality-reducing effects such as overheating cannot be quantified with common measurement methods, a qualitative assessment of the samples is done with a pairwise comparison

Figure 3 Austenitic steel 316L, arbitrary chosen powder particles of both powders

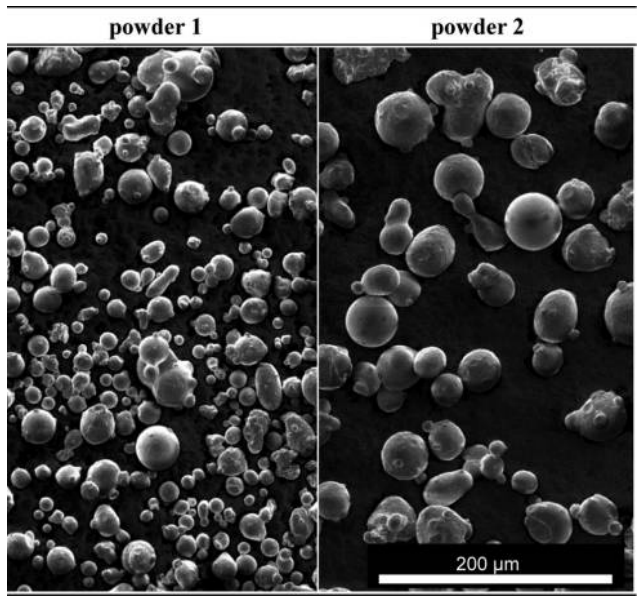

Figure 2 Particle size and volume distribution of austenitic steel Powder 1 and 2

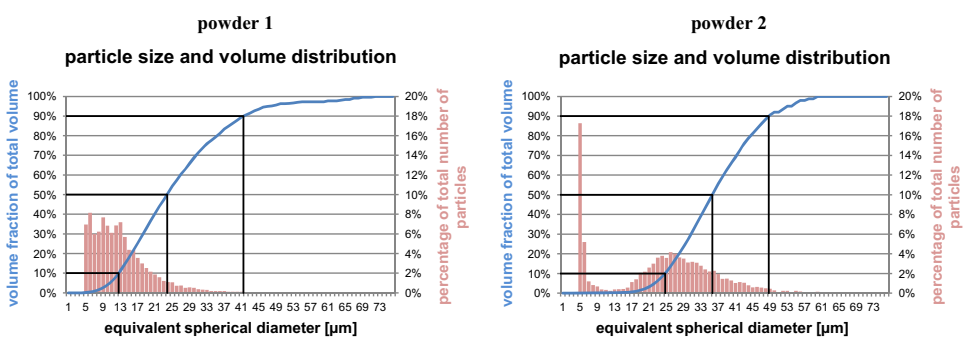

Figure 4 Left: results of the first test series realized with Powder 1 at the ConceptLaser M2, Right: results of the 25° samples visualized as the model of second order

process parameters				results					visualised model (2nd order) based on 25°
	h	α	v_s					Y	
sample	hatch distance	scan angle	scan speed	surface quality Ra 30°	25°	20°	density	over. impr. 25°	
[No.]	[mm]	[°]	[mm/s]	[µm]	[µm]	[µm]	[%]	[rank]	
1	0.08	90	1'500	23	--	--	89.2	16	
2	0.05	0	2'500	17	17	18	94.2	2	
3	0.065	45	2'500	23	22	--	90.1	12	
4	0.05	90	1'500	22	--	--	97.2	14	
5	0.05	45	2'000	25	23	--	95.6	7	
6	0.065	45	1'500	24	21	--	97.2	5	
7	0.08	45	2'000	21	--	--	92.6	13	
8	0.065	45	2'000	22	20	--	95.1	11	
9	0.065	0	2'000	14	17	19	95.1	3	
10	0.065	90	2'000	20	16	--	95.1	15	
11	0.065	45	2'000	22	16	--	95.1	10	
12	0.08	0	2'500	13	18	20	86.9	1	
13	0.08	90	2'500	18	--	--	86.9	8	
14	0.05	0	1'500	16	21	--	97.2	9	
15	0.05	90	2'500	20	16	--	94.2	6	
16	0.08	0	1'500	14	16	19	89.2	4	

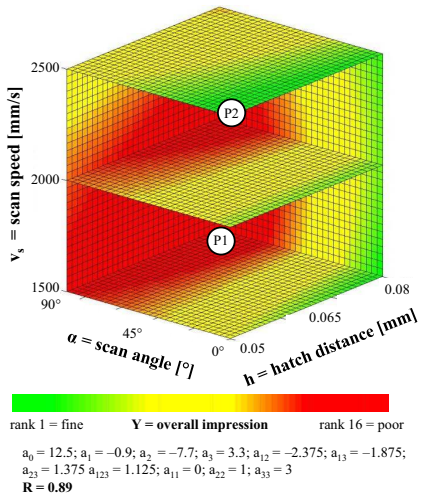

to rank the overall impression of the samples by numbers from 1 to 16. The results of the pairwise comparison serve to determine the significance of the used process parameters and scan strategy.

The overall impression results (Y = rank) derived from the pairwise comparison are transferred into a model of second order and will be expressed according to the process parameters to the following relation in equation (1):

$$\begin{aligned} Y &= a_0 && \text{Constant} \\ &+ a_1 h' + a_2 \alpha' + a_3 v_s' && \text{First order} \\ &+ a_{12} h'\alpha' + a_{13} h' v_s' + a_{23} \alpha' v_s' + a_{123} h'\alpha' v_s' && \text{Interactions} \\ &+ a_{11} h_2' + a_{22} \alpha_2' + a_{33} v_s' && \text{Second order} \end{aligned} \quad (1)$$

where h', α' and v_s' represent the normalized values of the parameters h, α and v_s, respectively. After normalizing, the minimum value (50 μm, 0° and 1,500 mm/s) equates to the value -1 and the maximum value equates to 1. From the combination of the coefficients and the normalized values, the dimensionless quantity rank (Y) is derived, which reflects the quality of the resulting sample.

The determination of the various coefficients a_i of the model is conducted by the least square method.

4.2 Test Series 2: minimum shell thickness $t_{s.min}$

The objective of the Test Series 2 is to derive the required minimal shell thickness $t_{s,min}$ by using the most promising parameter set of Test Series 1. The dense core of the segmented sample is produced with a standard parameter. This is done using samples as shown in Figure 1. The shell thickness $t_{s,min}$ is varied until the additive production of an defect-free sample is possible.

This test series is also conducted at the ConceptLaser M2 in combination with Powder 1. Additionally, this series is repeated by experiments with Powder 2. Finally, the tests based on both powders to determine the minimum shell thickness $t_{s,min}$ are also adopted on a comparable SLM system, namely, Renishaw 250. Because of the fact that two powders are tested at two different facilities based on the results of Test Series 1, possible influences on the results of the minimum shell thickness $t_{s,min}$ can be linked directly to the different powder particle distributions or used SLM systems. Selected shell-core samples are prepared for microstructural investigations.

5. Results

5.1 Test Series 1: parameter for minimum overhang angle φ_{min}

Up to an overhang angle φ of 30°, all 16 samples defined by the DOE were built successfully, independent of the process parameters used. In test series with an overhang angle of 25° or less, not all process combinations performed to high qualitative samples. For φ = 25°, four samples were of such poor quality that a measurement of the sample surface on the overhanging side was not possible (Figure 5, Sample P1). Because the quality range is huge within the 25° test series, the samples of this test series are ideally suited to determine the influence of the process parameters hatch distance, scan angle and scan speed.

Figure 4 shows the results of the qualitative assessment, which are transferred into a polynomial of degree 2 and visualized in a three-dimensional graph.

Through the three-dimensional representation of the results, it is obvious that the scan angle α has the most significant impact on the sample quality and that the best results are achieved at scan angles of 0°. The best results are obtained when using a scan angle of 0°, equivalent to a contour scan, because here the melt pool heat is conducted down to previously built layers and laterally to previously consolidated tracks. In case of the 90° scan angle, the heat is dissipated almost exclusively downward; thus, when using this scanning strategy, the risk of thermal accumulation is considerably larger. In addition, the resulting residual stresses significantly influence the feasibility of an overhang. Vrancken *et al.* (2013) demonstrates that the longitudinal residual

Figure 5 Examples of samples to illustrate the range of results

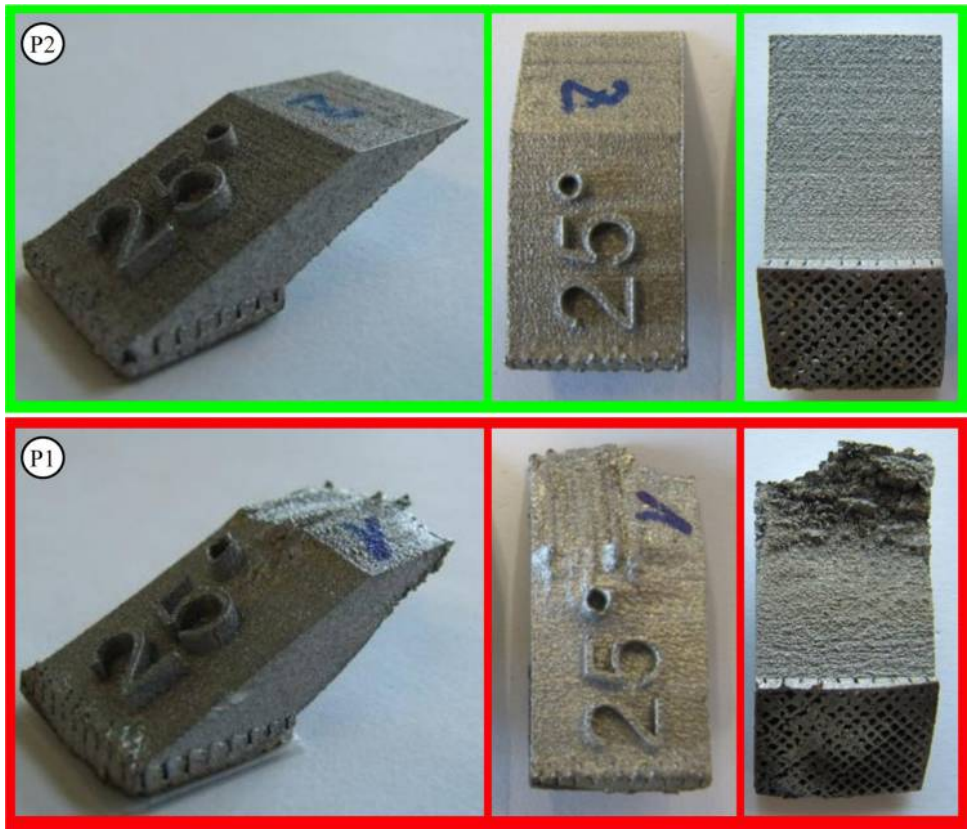

stresses in a scan track are significantly higher than the transversal residual stresses. This explains why deformations and poor quality occur earlier when using the 90° scan strategy compared to the 0° scan strategy.

With regard to the scan speed v_s, it can be stated that the minimum overhang and its quality can be improved by increasing the scan speed. This corresponds to the expectations where a low energy input is expected to have a positive impact on the overhang results because of less heat that has to be dissipated. The hatch distance h seems to have no significant influence within the investigated range.

The achieved surface qualities by using a scan angle of 0° lie between R_a = 13 and R_a = 21 μm, see also Figure 6. Not only the best surface qualities are obtained with the scan angle of 0° but also the only possibility to realize overhang angles of 20°. The measured sample densities are between 86.9 and 97.2 per cent.

The special feature of the 20° overhang sample is that the thermal cycles in case of the 0° and 90° scan strategies are comparable because of the identical edge lengths a and b. Because the 20° overhang samples could only be realized with the 0° scan strategy, it can be concluded that this scan strategy is much more suitable. However, it should be taken into account that the realization of the overhang surface depends strongly on the length of the scan track. As already pointed out, heat accumulation of two adjacent scan tracks is significantly influenced by the scan track length.

5.2 Test Series 2: minimum shell thickness $t_{s.min}$

The preliminary studies show that those scan strategies are the most suitable where the laser exposure is parallel to the overhanging contour. By using the contour scan, this strategy can simply be realized with the existing software architecture at both machine systems. So, the shell of the sample is realized by numerous contour scans, and the core is processed with standard parameters. Also, here it is important to consider that the scan process of the shell starts with the inner contour to ensure the maximum heat conductivity. The exposure of the shell is conducted immediately after the core exposure.

Figure 6 Surface quality as a function of the scan angle and the overhang angle

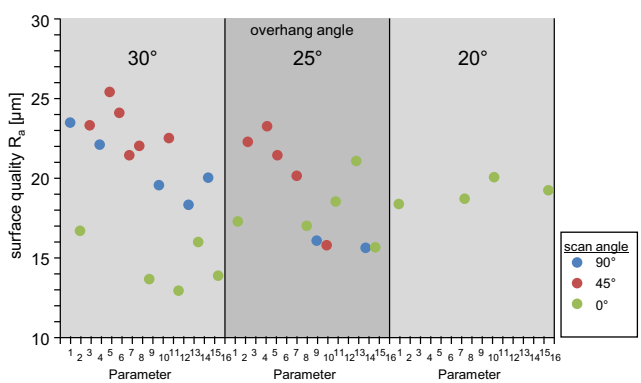

Because of technical constraints, scan speeds higher than 2,000 mm/s cannot be realized at the Renishaw system. According to this, Parameter 9 of Test Series 1 is adopted for the shell-core strategy within Test Series 2. This parameter corresponds to a volume energy of 51.3 J/mm^3 and a density of 95.1 per cent at a scan speed of 2,000 mm/s.

The quality of the samples by Test Series 2 shows that good results from the investigations of the minimum overhang angle within Test Series 1 are only transferable in a limited way. Samples free of deformation and overheating effects at an overhang angle of 35°, produced with the ConceptLaser M2, are only realizable with a thickness $t_{s,min}$ of 1.625 mm, corresponding to 25 contour scans. With decreasing overhang angles, the minimum thickness $t_{s,min}$ increases. An overhang angle of 30° is only possible at a minimal shell thickness $t_{s,min}$ of 2.275 mm, corresponding to 35 contours. Comparable overhangs as manufactured with the ConceptLaser M2 can also be produced with the Renishaw system. In general, the Renishaw system requires five fewer contours, corresponding to 0.325 mm, to adopt the overhang parameters on the shell-core strategy as shown in Figure 7. However, it was not possible to realize overhang angles below 30° when using the Renishaw system. At both SLM systems independent of the powder choice, the investigations about the correlation of shell thickness and overhang angle were aborted at 30°. At overhang angles smaller than 30° in combination with the shell-core strategy, the shell has to be dimensioned with a thickness of several millimeters. Thus, the shell loses its shell character because for fine or complex components, the overhanging structure is under the dimension of the necessary shell thickness.

The achieved surface quality of R_a = 14 μm by using Parameter 9 at an overhang angle of 30° in Test Series 1 could not be repeated in Test Series 2 by using the same parameter for the shell at the same overhang angle. Here, a R_a of 29 μm is possible. In general, the obtained surface qualities of Test Series 1 cannot be repeated at the segmented samples of Test Series 2.

It should also be mentioned that independent of the SLM system used, better results were always achieved when using Powder 2. Because of the fact that both powders are SS316L, the bi-modal particle size distribution in Powder 2 influences significantly the overhang surface quality. In Figure 8, an overview of different overhang sections is shown. This gives an idea about the porosity in the shell structures as well as the achieved surface qualities.

Figure 7 Parameters and minimum shell thickness $t_{s,min}$ to realize certain overhang situations at samples produced with a dense core at the Renishaw AM 250 and ConceptLaser M2 in combination with two different SS316L powders

test series 2			*results*	
sample	*machine*	*powder*	*ts*	*Ra*
overhang angle 35°			***[mm]***	***[µm]***
1	Concept	1	1.625	26.7
2	Concept	2	1.625	24.6
3	Renishaw	1	1.3	21.5
4	Renishaw	2	1.3	17.5
overhang angle 30°				
5	Concept	1	2.275	28.9
6	Concept	2	2.275	25.5
7	Renishaw	1	1.95	27.3
8	Renishaw	2	1.95	23.6

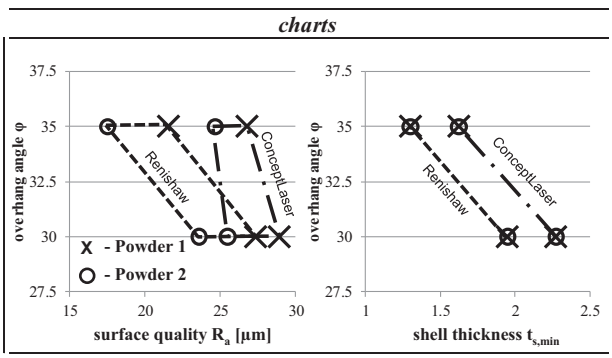

Figure 8 Comparison of selected light microscopic microstructure images in the region of the overhang to clearly see the porous structure of the shell

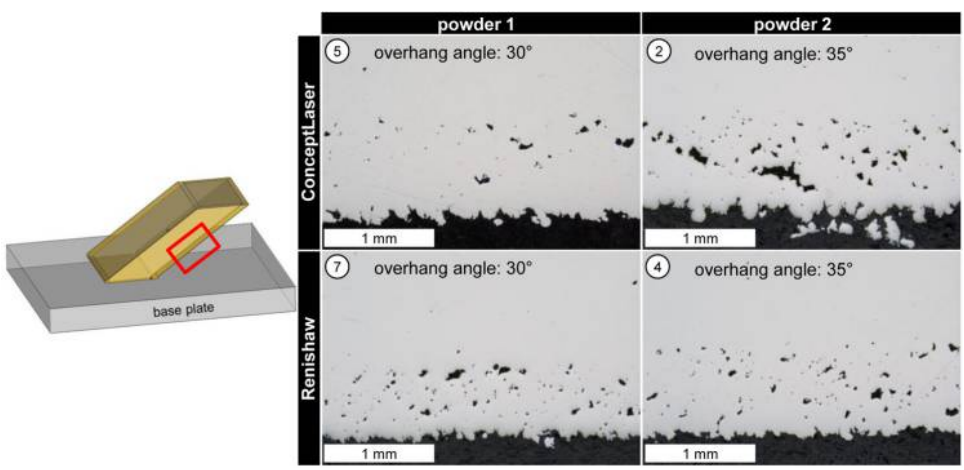

Figure 9 Illustration of the influence of the core process parameter on the smallest possible overhang angle even at a shell thickness larger than 1 mm

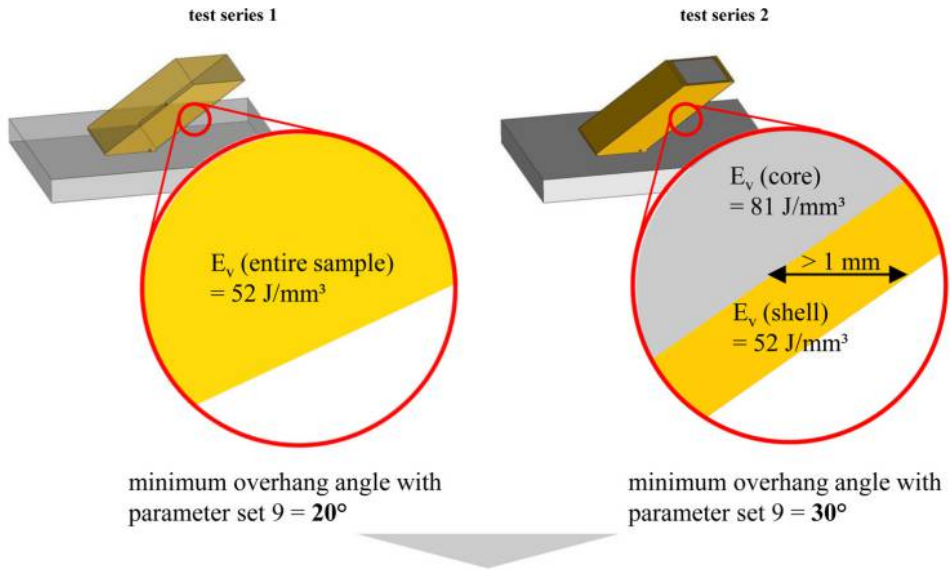

6. Conclusion and outlook

The results show that the SLM technology is able to realize support-less overhanging surfaces by choosing suitable scan strategies and process parameters. Particularly good results are always obtained when the exposure direction is parallel to the contour of the sample. However, repeating the good results of Test Series 1 by applying the most promising parameter set to a segmented sample is only possible in a limited way. Realizing overhang angles less than 35° is only possible with high shell thicknesses in the range of millimeters. However, the necessary shell dimension is not desired and not always accepted as the shell is coupled to high porosity (Figure 8). Therefore, this strategy can be applied to SLM components where mechanical strength is only of minor importance.

A direct comparison between the smallest possible overhang angle of Test Runs 1 and 2 when using the same parameter (Parameter 9) shows how strongly the critical overhang angle is influenced by the high volume energy E_v for producing a dense core (smallest possible overhang angle in Test Series 1 is 20° compared to 30° in Test Series 2). The scenario is illustrated schematically in Figure 9. The sample on the left-hand side is produced with Parameter 9, resulting in E_v = 52 J/mm^3. The sample on the right-hand side uses the core-shell strategy with the same E_v. Thereby, the core is produced with a standard parameter, resulting in a volume energy of 81 J/mm^3. Because only a 30° overhang is possible with the core-shell strategy, it becomes clear how strongly the volume energy of the core parameter affects the shell and overhanging surface even if it has a minimum thickness of more than 1 mm.

The results of the minimum layer thickness $t_{s,min}$ and the surface quality point out two interesting correlations.

The surface quality achieved using Powder 2 is significantly better than that achieved using Powder 1 and is independent of the machine used. However, further investigations on the particle size distribution and its influence on sample quality are necessary.

Generally speaking, the Renishaw system exhibits an overall better sample quality, namely, in terms of minimum shell thickness and surface quality compared to the ConceptLaser system (see Figure 7). This, however, requires further in-depth analyses and better understanding of the impact of pulsed laser operation on the resulting part quality.

References

Averyanova, M. and Bertrand, P. (2009), *Direct Manufacturing of Dense Parts From Martensitic Precipitation Hardening Steel Gas Atomized Powder by Selective Laser Melting (SLM) Technology*, *Innovative Developments in Design and Manufacturing*, CRC Press.

Buchbinder, D., Schleifenbaum, H., Heidrich, S., Meiners, W. and Bültmann, J. (2011), "High power selective laser melting (HP SLM) of aluminum parts", *Physics Procedia*, Vol. 12, pp. 271-278.

Chivel, Y. and Smurov, I. (2010), "On-line temperature monitoring in selective laser sintering/melting", *Physics Procedia*, Vol. 5, pp. 515-521.

Cloots, M., Spierings, A. and Wegener, K. (2013), *Thermomechanisches Multilayer-Modell zur Simulation von Eigenspannungen in SLM-Proben*, Tagungsband Simulationsforum 2013: Schweißen und Wärmebehandlung, Weimar, pp. 59-69.

Gedda, H., Powell, J., Wahlström, G., Li, W.-B., Engström, H. and Magnusson, C. (2002), "Energy redistribution during CO2 laser cladding", *Journal of Laser Applications*, Vol. 14, pp. 78-82.

Gusarov, A.V., Malakhova-Ziablova, I.S. and Pavlov, M.D. (2013), "Thermoelastic residual stresses and deformations at laser treatment", *Physics Procedia*, Vol. 41, pp. 889-896.

Kruth, J.-P., Mercelis, P., Van Vaerenbergh, J. and Craeghs, T. (2007), *Feedback Control of Selective Laser Melting*, Katholieke Universiteit, Leuven.

Mercelis, P. and Kruth, J.P. (2006), "Residual stresses in selective laser sintering and selective laser melting", *Rapid Prototyping Journal*, Vol. 12, pp. 254-265.

Rickenbacher, L., Etter, T., Hövel, S. and Wegener, K. (2012), "High temperature material properties of IN738LC processed by Selective Laser Melting (SLM) technology", *Rapid Prototyping Journal*, Vol. 19, pp. 282-290.

Sih, S.S. and Barlow, J.W. (2004), "The prediction of the emissivity and thermal conductivity of powder beds", *Particulate Science and Technology*, Vol. 22, pp. 427-440.

Thijs, L., Verhaeghe, F., Craeghs, T., Humbeeck, J.V. and Kruth, J.-P. (2010), "A study of the microstructural evolution during selective laser melting of Ti–6Al–4V", *Acta Materialia*, Vol. 58, pp. 3303-3312.

Vrancken, B., Wauthlé, R., Kruth, J.-P. and Van Humbeeck, J. (2013), "Study of the influence of material properties on residual stress in selective laser melting", *Proceedings of the Solid Freeform Fabrication Symposium*, *Austin*, *TX*, pp. 393-407.

Wang, D., Yang, Y., Yi, Z. and Su, X. (2013), "Research on the fabricating quality optimization of the overhanging surface in SLM process", *The International Journal of Advanced Manufacturing Technology*, Vol. 65, pp. 1471-1484.

Zaeh, M. and Branner, G. (2010), "Investigations on residual stresses and deformations in selective laser melting", *Production Engineering*, Vol. 4, pp. 35-45.

Corresponding author

Michael Cloots can be contacted at: michael.cloots@irpd.ch